FREESTYLE NON-GUIDED TRUE-ANATOMICAL BIOMETRICS: A FUSION OF HAND GEOMETRY AND TEXTURE FEATURES

A. M. Badawi[1], S. A. El-Naggar[2], M. S. Kamel[2]
[1]Biomedical Engineering Department, University of Tennessee, Knoxville, TN, USA
[2]Systems & Biomedical Engineering Department, Cairo University, Egypt
e-mail: ambadawi@utk.edu

Abstract - **This paper presents a freestyle non-guided-anatomical hand biometric system based on fusion of hand geometry and texture features. The system uses a photographic CCD camera or IR camera to capture hand images. The captured data is freestyle where no hand control guides or pegs are used. Captured images are first preprocessed, and then geometric hand features are extracted. Geometric hand features include: finger lengths, areas, circumferences, and widths. Images are then analyzed for the textural patterns on the back of the hands. Texture features of first and second orders statistics are extracted. Geometric and texture features are used to construct a feature vector. Performance statistical parameters are found to exceed 99.8%. This encouraging result suggests fusion of the texture information for the back of the hand together with other geometric features for hand biometrics authentication.**

***Keywords*- Hand geometry, texture features, biometrics, image processing, statistical measures, algorithms**

I. INTRODUCTION

Biometric recognition refers to the automatic recognition of individuals based on their distinguishing physiological and/or behavioral characteristics (biometric identifiers).

It associates/disassociates an individual with a previously determined identity/identities based on how one is or what one does. Common physiological biometrics includes face, eye (retina or iris), fingerprints, hand geometry, hand veins and thermal images. Behavioral biometrics includes voice prints, handwritten signatures and keystroke/signature dynamics. The ideal biometric would be easy to use, fast, noninvasive, convenient and socially acceptable [1].

Hand biometrics is the underlying foundation of modern biometrics by virtue of its 20-year history of live applications [1-11]. Hand geometry has several strengths and can be used to evaluate the majority of the working population. The measurements are rapid and safe for the user, and utilize a relatively simple method of sensing, which does not impose excessive requirements on the imaging optics [4]. Also, the amount of data required to uniquely identify a user in a system is the smallest by far, allowing it to be used with smart cards easily. Also, it is quite resistant to attempts to fool the system. The time and energy required to sufficiently emulate a person's hand is generally too much to be worth the effort, especially since it is generally used for verification purposes only. Further, hand geometry is ideally suited for integration with other biometrics, in particular, fingerprints. For instance, an identification/verification system may use fingerprints for infrequent identification and use hand geometry for frequent verification. It is not difficult to conceptualize a sensing system which can simultaneously capture both fingerprints and hand geometry. There are preexisting hand geometry verification systems, but they suffer from the following: Firstly, pegs are used to guide and control the position of hand on the board. These pegs leave impressions on the skin of the hand and may alter measured dimensions. Also, persons suffering from arthritis may find difficulty in positioning their hands in the unit. Enrollers should train users during the enrollment process and correct potential errors before they occur. Successful and correct enrollment may require demonstration and user training [1]. Secondly, measurements are taken along fixed axes in spite the size of the hand and do no take into account any anatomical landmarks. Hence when we compare the measurements of two hands there is no anatomical correspondence. Thirdly, they do not take advantage of non-geometric attributes of the hand, e.g., color of the skin [4]. Despite a recent literature [19-22] which proposes a non-guided method for localizing fingers tips and valleys and for geometric features extraction similar to our proposed algorithm started in 1999 [17-18, 9], we have been researching the freestyle hand geometry systems since 1999 [17-18,9]. We introduced its algorithm idea for non peg guided finger tips and valleys localization in the polar coordinates. The details of the algorithm were published in 2001 in the master thesis [9] initiated in 1999 and supervised by the principal author of this work. In this paper, we propose the feasibility of the fusion of texture features of the back of hand and the true anatomical geometric features for hand biometric authentication.

II. HAND BIOMETRIC SYSTEM

The hand geometry scanner uses a charge coupled device (CCD) camera to record the hand's image.

The authentication process can be summarized as follows:

- Enrollment phase:

a) The user places the right hand in the reader (device capturing the hand image) three times.

b) The unit's internal processor and software convert the hand image to a mathematical template, which is the average of the three readings.

c) The user's template may reside in internal memory, or on other media such as a hard disk.

- Operation phase:

a) The user places the right hand in the reader

b) The system compares the measurements of the user's hand to the template recorded during an enrollment session.

c) If the template and the hand match, the scanner produces an output--it may unlock a door, transmit data to a computer, verify identification, or log the person's arrival or departure time.

III. Image Acquisition and Features Extraction

2D images of the hand were captured with a CCD camera, and were calibrated and processed with our previously published method [23]. This method performs multiple preprocessing steps to form a contour of the hand. The contour can then be converted into polar coordinates in order to determine the maxima and minima of the hand. From this information, a total of 44 points can be determined, as seen in figure 1. A total of 29 features of the hand can be measured using these points.

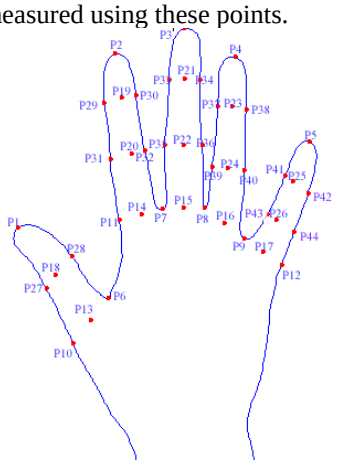

Fig.1. Automatically detected 44 point hand model

TABLE I
THE EXTRACTED GEOMETRIC FEATURES AND ITS DESCRIPTION

F	Feature Description	How to measure it
F1	Length of the thumb finger	Distance between P1&P13
F2	Length of the index finger	Distance between P2&P14
F3	Length of the middle finger	Distance between P3&P15
F4	Length of the ring finger	Distance between P4&P16
F5	Length of the little finger	Distance between P5&P17
F6	Width of the base of the thumb finger	Distance between P10&P6
F7	Width at 51%of the length of the thumb finger from the base	Distance between P27&P28
F8	Width of the base of the index finger	Distance between P11&P7
F9	Width at 38%of the length of the index finger from the base	Distance between P31&P32
F10	Width at 72.5%of the length of the index finger from the base	Distance between P29&P30
F11	Width of the base of the middle finger	Distance between P7&P8
F12	Width at 35%of the length of the middle finger from the base	Distance between P35&P36
F13	Width at 72%of the length of the middle finger from the base	Distance between P33&P34
F14	Width of the base of the ring finger	Distance between P8&P9
F15	Width at 33%of the length of the ring finger from the base	Distance between P39&P40
F16	Width at 70%of the length of the ring finger from the base	Distance between P37&P38
F17	Width of the base of the little finger	Distance between P9&P12
F18	Width at 28.5%of the length of the little finger from the base	Distance between P43&P44
F19	Width at 64%of the length of the little finger from the base	Distance between P41&P42
F20	The circumference of the thumb finger	Along the boundary from P10-P6
F21	The circumference of the index finger	Along the boundary from P11-P7
F22	The circumference of the middle finger	Along the boundary from P7-P8
F23	The circumference of the ring finger	Along the boundary from P8-P9
F24	The circumference of the little finger	Along the boundary from P9-P12
F25	The square root of the area of the thumb	
F26	The square root of the area of the index	
F27	The square root of the area of the middle	
F28	The square root of the area of the ring	
F29	The square root of the area of the little	

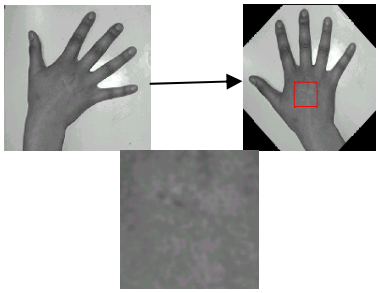

Fig.2. Shows the gray scale hand image, the hand image after rotation, the region of interest.

Figs. 2 and 3 show the strategy used to define the region of interest (ROI) of the hand to extract the texture features. Distance L shown in the image is half the distance between point P11 and point P9 shown in Fig 4. A perpendicular line of length L at the midpoint gives the center of the squared ROI of size L*L.

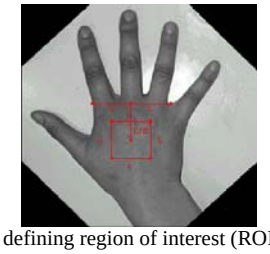

Fig.3. Strategy for defining region of interest (ROI) of the hand to get texture features.

From this analysis, we can add a total of 13 texture features, which are illustrated in Table II.

TABLE II
THE EXTRACTED TEXTURE FEATURES

Feature No.	Feature Description
F30	Mean
F31	Standard deviation
F32	Skewness
F33	Kurtosis
F34	Energy
F35	Entropy mode
F36	Autocorrelation
F37	Covariance
F38	Inertia
F39	Absolute value
F40	Inverse difference
F41	Energy of the second degree
F42	Entropy mode of the second degree

IV. Dataset

The dataset contain 500 images of hands for 100 distinct persons of both genders ranging in age from 16-35. The images were acquired under different lighting conditions, hand poses, intervals. The user places his/her right hand, palm facing downwards, on the surface of the device. He/She places his/her hand freely since there are no pegs or any guiding marks. An image of the top view of the hand is captured by a CCD camera. The size of each image is 640*480, 24-bit RGB. Five images of the same hand were

taken in succession. The user removes his hand completely from the device before every acquisition.

V. Results

We used 300 images as the training set, with three images for each person to compute the template of this hand. This template is computed simply by averaging the individual values of the feature vectors extracted from each image of the three. The remaining 200 hand images are used as the testing set. First, the normalized error between the template stored in the system's database and the input test hand is calculated as follows:

$$\text{Normalized error} = \frac{\| error \|}{\| temp \|} \quad (1)$$

$$\|\text{error}\| = \sqrt{\sum_{i=1}^{n} a(i) * (test(i) - temp(i))^2} \quad (2)$$

$$\|\text{temp}\| = \sqrt{\sum_{i=1}^{n} a(i) * (temp(i))^2} \quad (3)$$

Where n is the number of features and $a(i)$ is the weight of feature i. Then, the normalized error is compared with certain threshold. If the error is less than the threshold, then the test hand will be verified as the hand of the claimed identity; otherwise the test hand does not belong to the claimed identity. A decision made by the hand verification system is either a *genuine individual* type of decision or an *imposter* type of decision. Each type of decision may turn out to be either true or false. These different terms were computed for the system over different thresholds. We found that the maximum efficiency of the system was 99.135% at threshold 0.035 using the 42 geometric and texture features grouped. The system was tested using the 29 geometric features only at different thresholds. It was found that the maximum efficiency of the system is 99.115% at threshold 0.026. At this threshold the FAR was found to be 0.02% and the FRR was found to be 8.65%. The system was also tested using the 13 texture features only at different thresholds and it was found that the maximum efficiency for the system was 99% at a threshold of 0.0008.

A. Features Analysis for Biometrics

An analysis of these 42 features is of great use in determining the significance of individual features in biometrics applications and in robustness of our generated 3D models. Verification procedure can be greatly simplified and performed more rapidly if a classification can be made at high accuracy based upon only a few of the 42 extracted features. First feature coefficient of variation was calculated for each 5 samples/subject then averaged overall subjects and finally the coefficient of variation for the whole geometric features was found to be 1.4% with a standard deviation of 0.6%. To determine the robustness of our features, 300 images in the dataset were used to train the classifiers, and then the remaining 200 images were used to test the classifiers. The matching done here is a normalized error between the template vector and the test one. The features' significant power was ordered using the fisher discriminate ratio. The features were then ranked in descending significance order. In order to get the best verification rate, the system was optimized by plotting the biometric performance vs. the number of features and threshold. The best efficiency of performance was 99.61 % utilizing 14 features at a threshold of .0152 as shown in Fig 4. Fig. 4 shows the system performance as a function in number of features and threshold and the most significant features identified from the ranking procedure.

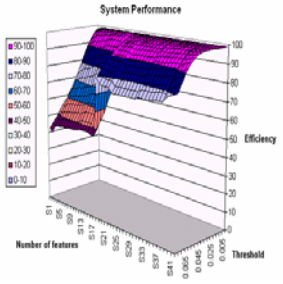

Rank	Feature#	Feature Description
1	F4	Length of the ring finger
2	F3	Length of the middle finger
3	F5	Length of the little finger
4	F12	Width at 28%from base of middle finger
5	F2	Length of the index finger
6	F9	Width at 27.5% from base of index finger
7	F10	Width at 62% from base of index finger
8	F16	Width at 67% from base of ring finger
9	F13	Width at 65% from base of middle finger
10	F15	Width at 30% from base of ring finger
11	F7	Width at 51% from base of thumb finger
12	F40	Difference
13	F39	Absolute value
14	F38	Inertia

Fig.4. The system performance is optimized and the most significant features are identified.

From these results, the lengths of the fingers seem to be the most significant features in classifying the hand geometry. The widths of the knuckles are also shown to be significant. The thumb length is not a very robust feature, as its rank was 24. This was expected because when the user places his hand with varying angles between the fingers, the location of the minima point is highly affected by the angle between thumb and index fingers. The other minima points are not affected by the angle as long as the user opens his/her fingers. We now have robust measures for the segments and texture features.

B. Features Fusion and Categorization

Another approach was used by putting the features in categories according to their units and types. As mentioned before, the feature vector consists of 42 features (29 geometric and 13 texture). As all the geometric features (lengths of fingers, widths of fingers, circumference of fingers and square root of the area of the fingers) are lengths, we can put them all in one category. The texture features are of different units so each feature is a category. This results in 14 categories of features. The global cost is calculated as follows:

$$C_G = \frac{\sum_{i=1}^{n} a_i c_i}{\sum_{i=1}^{n} a_i} \quad (4)$$

$$c_i = \frac{\| template - test \|}{\| template \|} \quad (5)$$

For the 14 categories C_G will be:

$$C_G = \frac{a_1 \sum_{i=1}^{29} c_i + \sum_{i=30}^{42} a_i c_i}{a_1 + \sum_{i=30}^{42} a_i} \quad (6)$$

a_1 is the coefficient of the first category, which represents the geometric features.

C. Features Fusion Weighting

The global cost C_G needs to be minimized for maximum similarity between unknown vectors and the stored template. Normally the coefficients in the equation are of equal weights and equal to one. Since there is a degree of significance for each feature with respect to others, we tried to get the optimal weights that maximize the correct verification, which is a simple linear optimization problem. What is the weight $a(i)$ that maximizes the correct verification? The problem is that for a relative weight from 1 to 10, we need (10^42) seconds of computation time to find the efficiency for each weights combination. It is about a second to calculate the efficiency for each weight combination. Thus it needs about 3.17*(10^34) year to complete the calculations ((10^42)/(60*60*24*365)). The computation time calculations is based on P4 2.4 GHz, 256 MB RAM PC. First, trial & error was used for weighting the features. Then a Neural Networks as a nonlinear method of parallel optimization was proposed for features and categories weighting.

D. Features Categories Weighting Using Neural Networks

We used two different networks for weighting the features. The network consists of a first input layer, a second (hidden) layer of variable number of perceptrons feeding a third (output) layer [16]. The output is one if the unknown hand is correctly verified and zero if the unknown hand is not verified correctly. The number of the input nodes in the first network is 42, corresponding to all the geometric and texture features. The second network has 14 input nodes, corresponding to the 14 categories of features. There were 60000 vectors to train the network, which correspond to the normalized error between the 200 test hand image and 300 template stored in the system. The results are presented in table III.

TABLE III
NEURAL NETWORK RESULTS OF FEATURES WEIGHTING

NN Parameters	For 42 Feature	For 14 category
Number of input nodes	42	14
Number of nodes in hidden layer	60	25
Number of epochs	20000	15000
Mean square error	0.000821	0.000562
Momentum term	0.75	0.75
Learning factor	0.8	0.85
Goal	0.0001	0.0001
Error function	Tanch Sigmoidal	Tanch Sigmoidal
Percentage of matching	99.52 %	99.82 %
Time for network training	15 hours	8 hours

It was found that the maximum percentage of matching in the Neural Network analysis was 99.82% for 14 categories of features. So this percentage corresponds to the best weighting done by the Neural Network to different categories.

VI. CONCLUSION

The freestyle system was able to prove the viability of hand biometrics in medium security applications due to its ease of use and robustness. The efficiency of the system is quite high, and was only improved by the addition of the texture features. The freestyle approach allows for high ease of use as the subject does not have to worry about the orientation of their hand. Currently, we are studying several effects on the biometric process, including the effects of infra-red imaging, re-quantizing the gray level scale to 32 in the texture window, and integrating the hand information with other biometric modalities such as hand veins.

REFERENCES

[1] A. Jain, R. Bolle, and S. Pankanti, “Biometrics. Personal Identification in Networked Society”, Kluwer Acad. Publisher, 1999.
[2] A. Jain, A. Ross and S. Prabhakar, “An Introduction to Biometric Recognition1”, IEEE on Circuits and Systems for Video Technology, Special Issue on Image- and Video-Based Biometrics, Vol. 14, No. 1, January 2004.
[3] A. Jain, L. Hong, and S. Pankanti, ” Biometric Identification”, ACM, Vol. 43, No. 2, February 2000.
[4] A. Jain, A. Ross and S. Pankanti, ”A Prototype Hand Geometry-based Verification System”, 2nd Int'l Conference on Audio- and Video-Based Biometric Person Authentication (AVBPA), Washington D.C., pp.166-171, March 22-24, 1999.
[5] R. Sanchez-Reillo, C. Sanchez-Avila and A. Gonzalez-Marcos, ”Biometric Identification through Hand Geometry Measurements”, IEEE Transactions On Pattern Analysis and Machine Intelligence, Vol. 22, NO. 10 October 2000.
[6]“Individual Biometrics-Hand Geometry”, http://ctl.ncsc.dni.us/biomet%20web/BMHand.html
[7] “The Global trade association for automatic identification-Hand Geometry ”, http://www.aimglobal.org/technologies/othertechnologies/biometric_handgeometry.asp
[8] “Biometrics-Hand Verification”, http://biometrics.cse.msu.edu/hand_geometry.html
[9] Nader Abd El-Rahman, “Automatic Hand Geometry Verification System”, MSC thesis, Cairo University 2001.
[10]“Hand Geometry”, http://www.666soon.com/hand3.htm
[11]“FingerGeometry”,http://www.biometricwatch.com/Technologies/Finger_Geometry/Finger_geometry.htm
[12] “Image Processing Fundamentals”, http://www.ImageProcessingFundamentals/Segmentation.htm
[13] M. Sonka, V. Hlavac and R. Boyle, “Image processing Analysis and Machine Vision”, Chapman &Hall, 1993.
[14] Y. Kadah, A. Farag, J. Zurada, A. Badawi and A. Youssef, "Classification algorithms for quantitative tissue characterization of diffuse liver disease from ultrasound images", IEEE Trans. Medical Imaging, vol. 15, no. 4, pp. 466-478, August 1996.
[15] A. Materka and M. Strzelecki ,“Texture Analysis Methods- A Review”, Technical University of Lodz, Institute of electronics, COST B11 report, Brussles 1998.
[16] R. Beale and T. Jackson, “Neural Computing: An Intoduction”, IOP Publishing Ltd 1998.
[17] A. Badawi, M. Kamel, ”Freestyle Hand Geometry Verification System”, 46th IEEE Midwest Symposium on circuits and systems, 2003.
[18] A. Badawi, M. Elmahdy, K. Elsayed, ”A low-Cost and Pc-Based Automatic Hand Geometry Verification System”, In Proceedings of IEEE, International Conference on Industrial Electronics, Technology and Automation IETA, December, 2001.
[19] W. Xiong, C. Xu, S. Ong, “Peg-Free Human Hand Shape Analysis and Recognition”, II-77-II-80, ICASSP 2005.
[20] C. Han, H. Cheng, C. Lin, K. Fan,” Personal authentication using palm-print features” Pattern Recognition 36 (2003) 371 – 381.
[21] C. Lina, T. Chuangb, K. Fan,” Palmprint verification using hierarchical decomposition”, Pattern Recognition 38 (2005) 2639 – 2652
[22] W. Xionga, K. Toha,W. Yaua, X. Jiang,” Model-guided deformable hand shape recognition without positioning aids”, Pattern Recognition 38 (2005) 1651 – 1664.
[23] A. Badawi, M.R. Mahfouz, D. Holmes, “Rapid 3D Hand Modeling”, Computational and Computer Methods in Biomechanics and Biomedical Engineering, 2006.